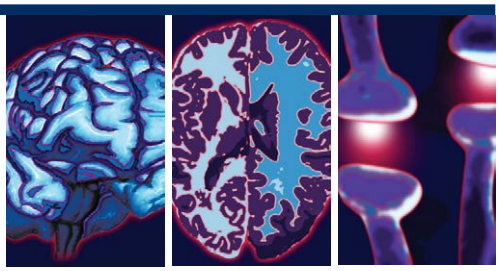

Social Buffering Prevents Stress-Induced Decreases in Dendritic Length, Branching in Dentate Granule Cells and Hippocampus-Related Memory Performance

Wen-Yu Tzeng[1,*], Tung-Yi Huang[1,*], Chianfang G Cherng[2], San-Nan Yang[3,^], Lung Yu[1,^]

Abstract

Objectives: A robust stressor regimen may cause a rapid decrease in BDNF level in the dentate gyrus (DG) while social buffering appears to prevent such decrease. Local BDNF levels and downstream phosphorylation of ERK and CREB play a critical role in mediating morphological and synaptic plasticity in DG. Thus, this study was undertaken to assess whether an acute stressor regimen may render morphological changes and whether the social buffering may prevent such changes in the existing DG granule cells. Moreover, we attempted to assess whether the stressor regimen and social buffering may also affect local ERK and CREB phosphorylation and the hippocampus-related memory.

Methods: Six hours after the conclusion of the stressor regimen, morphological indices of the granule cell in DG were obtained in Balb/C mice experiencing no stressor, the stressor regimen alone or in a group.

Results: The stressor caused significant decreases in the total length of dendrites, number of dendritic branches, and the size of the dendritic field in granule cells, while the social buffering prevented all these changes. Likewise, the stressor caused decreases in local ERK phosphorylation and object location performance, while the social buffering prevented such decreases of ERK phosphorylation and deteriorated memory performance.

Conclusion: These results, taken together, suggest that stress and social buffering may rapidly affect the existing DG granule cell morphology and hippocampus-related memory performance by modulating local ERK phosphorylation.

Keywords:

Dentate gyrus, Granule cell, Single-cell labelling, Stress, Social buffering

Introduction

A great deal of evidence indicates that stress and corticosterone (CORT) level can cause drastic morphological and synaptic changes in existing neurons in the hippocampus and such changes may serve for adaptive purposes for hampering ongoing apoptotic progression and/or facilitating eventual recovery and allostasis [1]. For example, adrenalectomy results in significant atrophy of CA3 pyramidal neurons [2]. Likewise, both repeated restraint and chronic multiple stressors cause atrophy of the apical dendrites of hippocampal CA3 pyramidal neurons [3]; this

[1]Department of Physiology, National Cheng Kung University College of Medicine, Tainan 70101, Taiwan, ROC

[2]Department of Health Psychology, Chang Jung Christian University, Tainan 71101, Taiwan, ROC

[3]Department of Pediatrics, E-Da Hospital, I-Shou University, Kaohsiung 82445, Taiwan

[†]Author for correspondence: Dr. Lung Yu, Institute of Behavioral Medicine, National Cheng Kung University College of Medicine, 1 University Rd., Tainan 70101, Taiwan, Tel: +886-6-2353535 ext. 5114, Fax: +886-6-2095616; email: lungyu@mail.ncku.edu.tw

*Both Contributed equally to the work.

^Co-corresponding authors for the article.

repeated restraint stressor-produced atrophy of the apical dendrites requires CORT secretion [4]. Moreover, chronic stress or repeated CORT injections may also cause atrophy of these same dendrites [3-7]. Although the survival of granule cells in the dentate gyrus (DG) is highly dependent on normal circulating CORT level [8], excessive glucocorticoid secretion does not seem to cause observable changes in the dendritic morphology of the DG granule cells [5]. The discrepancy in stress-produced morphological changes between CA3 pyramidal neurons and DG granule cells could arise from the timing of the observation, the actual CORT level, and/or species differences. Whether the existing DG granule cells are invariably resistant to stress and/or stress-induced CORT secretion remains unknown. We have reported that a stressor regimen including randomly scheduled, unavoidable foot shock delivery followed by restraint in water, produces robust and long-lasting increases (approximately 4-fold increase and lasting for 3 hours at least) in mouse serum CORT level [9]. Using this stressor model, we sought to determine if our intense stress-induced long-enduring CORT secretion may cause rapid changes in dendritic morphology of the DG granule cells.

In addition to the impact of the stressor regimen on CORT level, intense stressors are known to cause a decrease in local BDNF expression in mouse DG [10,11]. In contrast, the presence of three companions serving as social buffering appears to prevent the stress-induced decrease in local BDNF expression [10,11]. BDNF induction has been known to play a critical role in mediating morphological and synaptic plasticity in DG granule cells [12-14]. Moreover, BDNF is found to induce these morphological and synaptic changes likely via phosphorylation of local extracellular signal-regulated kinases (ERK) and ERK-dependent cAMP response element binding protein (CREB) phosphorylation [15-17]. Thus, the present study was designed to assess whether the present stressor regimen may cause changes in local ERK and CREB expression and phosphorylation in DG. Likewise, we attempted to examine whether the social buffering may prevent the stressor-induced changes in ERK and CREB expression and phosphorylation.

Both object recognition and location tasks are hippocampus-related and stress-free memory tasks [18-20]. Likewise, two versions of the Y-maze task, spontaneous arm alternation and exploration for the previously blocked arm, have been used to assess the quality of the hippocampus-related memory [21]. Hippocampal BDNF expression has been thought to modulate rodents' performance in the object location task [22]. In fact, many reports show that BDNF mRNA and protein expressions in the DG correlate positively with the performance of the object recognition task [23-25]. Moreover, recent studies depict the critical roles of hippocampal BDNF induction and the down-stream activation of ERK and CREB in the object recognition memory [26-29]. Importantly, a recent study reveals that granule cell morphology in the DG is closely linked to the performance of Y maze task in a rat model [21]. Thus, we decided to test the hypothesis that our stressor regimen and social buffering may affect the hippocampus-related memory performance in the object recognition, object location and Y maze tasks.

Materials and methods

All experimental procedures involving animals were conducted in accordance with the National Institutes of Health Guide for the Care and Use of Laboratory Animals (NIH Publications No. 80-23) revised in 1996. All the experimental procedures were approved by the Institutional Animal Care and Use Committee of National Cheng Kung University College of Medicine, Taiwan, ROC. The timelines for arranging the stressor procedure in the morphological, biochemical and behavioral experiments are listed in **Figure 1**.

■ Animals

Male Balb/C mice were bred at National Cheng Kung University College of Medicine Laboratory Animal Center. After weaning, Balb/C mice were group housed in plastic cages (28 x 17 x 12 cm, six per cage) in a temperature- and humidity-controlled colony room on a 12-h light/dark cycle with lights on at 07:00 h at the Center. Mice had access to food (Purina Mouse Chow, Richmond, IN, USA) and tap water *ad libitum*. All experiments started when mice reached 8 weeks of age.

■ The tandem stressor regimen

In this study, the tandem stressor regimen referred to a randomly-scheduled delivery of unavoidable foot shock (0.5 mA and a 1-sec duration each with an average of 1 shock/min

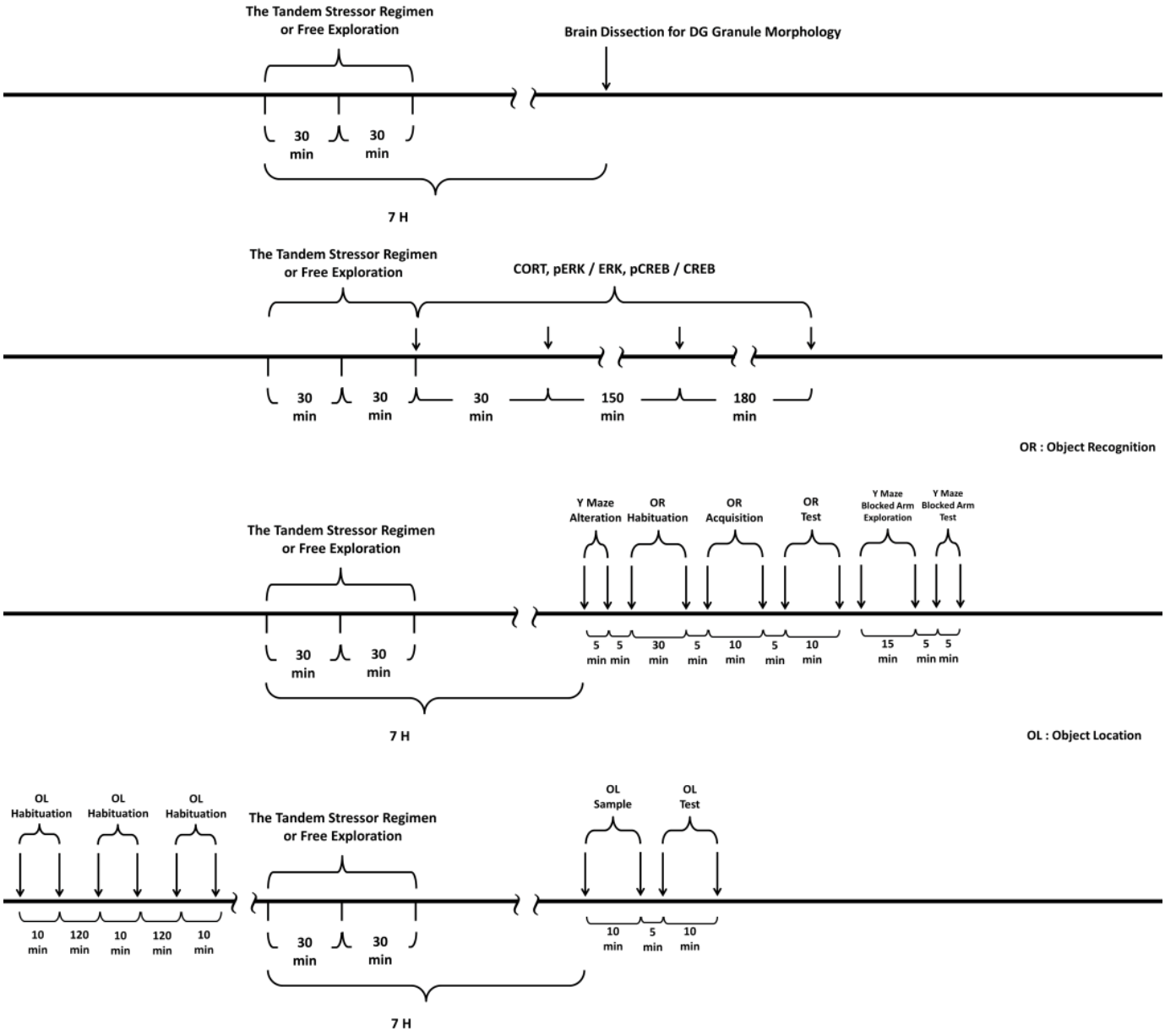

Figure 1: A schematic representation of experimental procedures.

for 30 min) in a 24-cm long, trough-shaped metal alley (for delivering foot shock) **(Figure 2)** immediately followed by a 30-min restraint in a one third-immersed plexiglas cylinder (7 cm in length and 3.4 cm in diameter for the top circle) within a plastic pan (31 x 23 x 7 cm) **(Figure 2)** [9,11].

■ Grouping and the experimental procedures

To study the effects of stress and social buffering on dendritic morphology of the DG granule cells, the phosphorylation of local intracellular signalling molecules, including ERK and CREB, and the performance of the hippocampus-related memories, three groups of mice were used. Unrestrained mice navigating the alley **(Figure 2a)** for 30 min and plastic pan for 30 min with a group of three companions (their cage mates) and being transferred to a clean plastic holding cage (47 x 26 x 21 cm) alone for 6 hours served as the "No stressor" group. Mice experiencing the stressor regimen in the alley and pan alone and being transferred to a clean plastic holding cage for 6 hours served as the "Stressor alone" group. Finally, mice undergoing the stressor regimen with a group of three companions (their cage mates) and being individually transferred

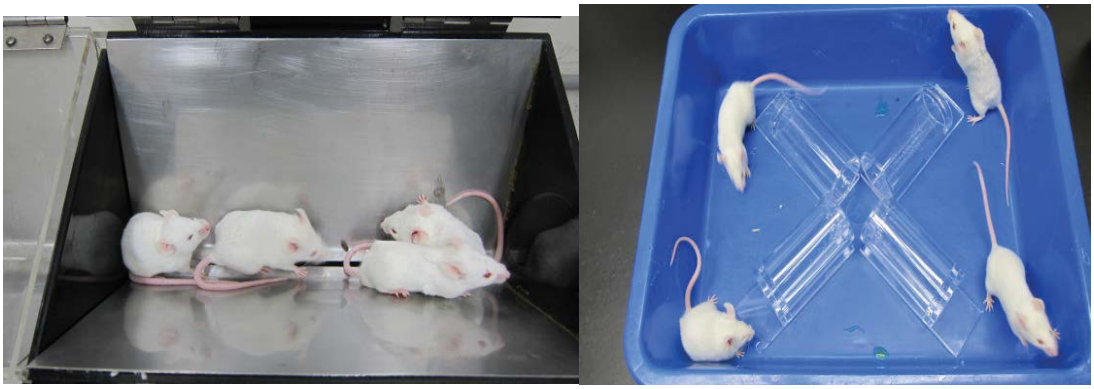

Figure 2: Photo representatives. Along with a group of three companions, unrestrained mouse demonstrators (a) navigate in the alley and (b) the dry pan.

to a clean plastic holding cage for 6 hours were used as the "Stressor in a group" group. A total of 36 mice [No stressor (N=12), Stressor alone (N=12), and Stressor in a group (N=12) group] were used. Since mice were originally housed 6/cage, two mice from each cage were not used in this study. Likewise, 24 randomly chosen mice from 6 cages (4 from each cage) were used for the "Stressor alone" and "Stressor in a group" for the morphological experiment. A total of 755 granule cells were successfully scored in the DGs in these mice. Specifically, the following numbers of cells were successfully identified and scored for individual mice in the "no stressor" (total=249; individual mice=25, 22, 22, 22, 22, 19, 19, 19, 20, 19, 20, 20), "stressor alone" (total=255; individual mice=25, 24, 19, 21, 22, 22, 21, 20, 20, 20, 20, 21), and "stressor in a group" (total=251; individual mice=25, 22, 20, 21, 23, 21, 19, 21, 19, 21, 20, 19). The timeline for the stressor procedure and the morphological experiment is presented in **Figure 1** (top panel).

In order to examine the impact of the stress-induced and social buffering effects on the phosphorylation of ERK and CREB in the DG, another set of 72 mice [No stressor (N=8), Stressor alone (N=32), and Stressor in a group (N=32)] were used. Two, eight, and eight cages of mice were used for the "No stressor", "Stressor alone" and "Stressor in a group" group, respectively. Mice of the "No stressor" group served as controls for revealing the phosphorylation baselines of ERK (pERK/ERK) and CREB (pCREB/CREB) in the DG tissue samples. At times of 0 hr (N=8), 0.5 hr (N=8), 3 hr (N=8), and 6 hr (N=8) after the conclusion of the stressor regimen, mice from the "Stressor alone" and "Stressor in a group" group were killed for the assays. The time line for the stressor procedure and this biochemical experiment is presented in **Figure 1** (second top panel).

To test the possibility that mouse serum CORT at 6 h after the conclusion of the stressor regimen may affect the hippocampus-related memory performance, a set of 56 mice were used. Mice were killed by rapid decapitation and their trunk blood was collected without exposure to the stressor (N=8), or at 30 min, 3hr, and 6 hr (for each time N=16, with 8 in the "Stressor alone" and 8 for the "Stressor in a group" groups) after the cessation of the stressor regimen. Two, six, and six cages of mice were used for the "No stressor", "Stressor alone" and "Stressor in a group" groups, respectively. The time line for the stressor procedure and CORT experiment is presented in **Figure 1** (second top panel). Finally, a total of 54 mice (26 for object recognition and Y maze task and 28 for object location task) were used for assessing the hippocampus-related memory performance. The timeline for the stressor procedure and behavioral experiments is listed in **Figure 1** (two bottom panels).

■ Dendritic measures of the DG granule cell

Mice were deeply anesthetized by using a mixed anesthetic (consisting of ketamine: 50 mg/ml, xylazine: 23.3 mg/ml, atropine: 1 mg/ml; 2 ml/kg; i.p.) to enable transcardial perfusion with artificial cerebrospinal fluid [117 mM NaCl, 4.7 mM KCl, 2.5 mM $CaCl_2$, 11 mM glucose, 1.2 mM $MgCl_2$, 25 mM $NaHCO_3$, 1.2 mM NaH_2PO_4, (pH adjusted to 7.4)] containing heparin (1,000 IU) followed by a fixative solution containing 4% paraformaldehyde and 4% sucrose in 0.1 M phosphate buffer (pH adjusted to 7.2). Brains were then removed and

post-fixed in the 4% paraformaldehyde and 4% sucrose solution at 4°C overnight and transferred to 0.1 M phosphate buffer before slicing. Brain slices containing the DG (from Bregma -0.94 to Bregma -3.5) were used. Using protein synthesis rate as an index of neuronal plasticity, subregion-dependent differences in plasticity are noticed in the DG [30,31]. To parcel out the plausible regional differences in the stress susceptibility of the DG granule cells, granule cells in the suprapyramidal blade, hilus tip, and infrapyramidal blade division were equally subjected to lucifer yellow labeling on each slice. If the granule cells were not completely labeled with the fluorescence dye and showing any evidence of dendritic cutting, the cells were discarded from further analysis. It was of interest to note that the successful rate of labeling the granule cells in the suprapyramidal blade was approximately two times greater than it was in the hilus tip or the infrapyramidal blade **(Table 1)**. Since no significant regional or sub-divisional differences were noticed in dendritic morphological analyses under control (no stressor), stressor alone or stressor in a group condition, region and subdivision variables were crashed for further analyses.

The single-cell labeling method was employed as previously described [32] with minor modification. In brief, a series of coronal section (200 μm thick) were made and a single section was transferred to an injection chamber mounted on the stage of a fluorescence microscope (Nikon E600FN, Nikon, Japan). The location of the cell body in the DG granular layer was viewed by the use of differential interference contrast optics under a 40 x objective lens (numerical aperture=0.8, water immersion). We decided to label existing granule cells with cell bodies located in the outer two-thirds of the granule cell layer for the best to avoid labeling the adult new-born immature granule cells [33]. Early-born granule cells at embryonic stage or early postnatal development are thought to have multiple primary dendrites, while late-born granule cells at adulthood usually present one or two primary dendrites [33]. Dendritic plasticity of adult granule cells is sensitive to experiences [34]. Since stress- and social buffering-induced morphological plasticity in DG granule cells at adulthood was concerned, only labelled granule cells with one or two primary dendrites were used for quantitative measurements. Cell bodies of single granule cells were iontophoretically labeled (1 Hz, -100 ~ -700 mV, 2-10 min labeling time per cell) using a lucifer yellow-filled micropipette (o.d. < 1 μm). Emergence of yellow fluorescence was monitored through a dichroic filter cube (EX450-490 nm, DM505 nm, BA520 nm). The excitation light was applied from a computer-controlled fast wavelength switcher (Lambda 10-2, Sutter Instruments, Novato, CA, USA), with exposure times 0.3-0.7 s per frame (275 μm × 275 μm). The images were acquired by a CCD camera (Cool Snap fx, Photometrics, AZ, USA) and processed using the Meta Fluor software (Molecular Devices, Sunnyvale, CA, USA). Image Z-stacks with vertical separation around 1-2 μm were obtained manually. The fluorescence intensity was quantified using an 8-bit (0-255) gray scale. The measurements were performed on projection-compressed images obtained from Z-stacks using the Maximum intensity projection type of the Grouped Z Projector function of ImageJ (version 1.46 p, Wayne Rasband, NIH, USA; http://rsb.info.

Table 1: The total number of labeled granule cells collected from the suprapyramidal, infrapyramidal blades, hilus tip subdivisions in the anterior, middle, posterior dentate gyrus (DG) among "No stressor", "Stressor alone", and "Stressor in a group" group.

	Subdivision	No Stressor	Stressor alone	Stressor in a group	Subtotal
Anterior DG (Bregma:- 0.94~-1.9mm)	Suprapyramidal blade	45	45	36	126
	Hilus tip	21	21	20	65
	infrapyramidal blade	18	20	22	59
	Subtotal=	**84**	**86**	**78**	**248**
Middle DG (Bregma:- 1.9~-2.7mm)	Suprapyramidal blade	40	38	44	122
	Hilus tip	19	21	17	69
	infrapyramidal blade	37	26	26	65
	Subtotal=	**86**	**85**	**87**	**258**
Posterior DG (Bregma:- 2.7~-3.5mm)	Suprapyramidal blade	41	42	41	124
	Hilus tip	18	19	19	67
	infrapyramidal blade	20	23	26	58
	Subtotal=	**79**	**84**	**86**	**249**
Subtotal		**249**	**255**	**251**	**Total: 755**

nih.gov/ij). After the 2D image of the dendritic field for each granule cell was constructed (Figure 3), its total dendritic length and branch points were obtained using the NeuronJ plug-in of the ImageJ neuronal tracing system. Likewise, Sholl analysis was conducted on the 2D images. To perform Sholl analysis, 10-μm increment concentric rings centering at the cell body were superimposed over the 2D image with the aid of the plug-in of "concentric circles" of the ImageJ software. The dendritic field, including the branch and length distribution of dendrites, was analyzed up to 30 concentric rings. The intersections of the dendrites and each ring were counted accordingly.

A custom-made two photon image system was used to examine dendritic spine density as previously described [32]. Dendritic spine density results from five randomly chosen granule cells with one primary dendrite in anterior (or dorsal) (from Bregma -0.94 to -1.9 mm) DG were averaged for each mouse in "No stressor" (N=12), "Stressor alone" (N=12) and "Stressor in a group" (n=12) groups. The dendritic spine of the labeled DG granule cell in anterior (or dorsal) DG was observed using a 63x objective lens (NA = 1.4, Oil DIC, Plan-APOCHROMAT, ZEISS, Oberkochen, Germany). Existing granule cells in DG are known to receive inhibitory modulation from local GABAergic neurons and at least two types of these GABAergic neurons form synapses with spines in proximal dendrites of the granule cells [35]. To understand stress- and social buffering-induced plasticity in dendritic spine density for these inhibitory synapses, consecutive optic sections (z-axis depth 20 μm, 0.5 μm each section) were taken at Sholl distance of 50~100 μm (centering at the soma) and a projected image (50 μm × 50 μm) was reconstructed. Following z-axis projection (3D converted to 2D), an average length of 90 μm was used for spine number quantification. We used the cell counter plugin of ImageJ software to manually count the spine number. The dendritic spine density was expressed as number of spine/10μm.

■ Stress-produced and social buffering effects on the phosphorylation of ERK and CREB in the DG

Western immunoblotting was used to determine relative levels of total ERK, CREB and phosphorylated ERK, CREB in the DG tissue samples. Mice were killed by rapid decapitation and their brains were removed and placed on the dorsal surface in mouse brain slicers sitting on crushed ice. Two coronal sections were made. The first and second coronal sections were cut at 4 mm and 2 mm anterior to the posterior bank of the cerebrum. A slab was obtained between these two sections. A horizontal cut was made between bilateral notches (rhinal fissures) in the slab and the bottom part of the slab was discarded. Under an anatomical microscope (Olympus SZ51, Tokyo, Japan), part of the thalamus and hippocampal CA region were removed from the top part of the slab and a portion of DG tissue, primarily consisting of anterior and middle portion of DG, was dissected out and used for assaying the phosphorylation extent of ERK and CREB. The DG tissue samples were homogenized in ice-cold lysis buffer containing protease inhibitor cocktail (Roche, Basel, and Switzerland). Homogenates were centrifuged at 12,000 × *g* for 10 min at 4°C, and the protein concentrations of supernatants were determined by Bradford method (Bio-Rad Protein Assay, BioRad Laboratories, Hercules, CA, USA)

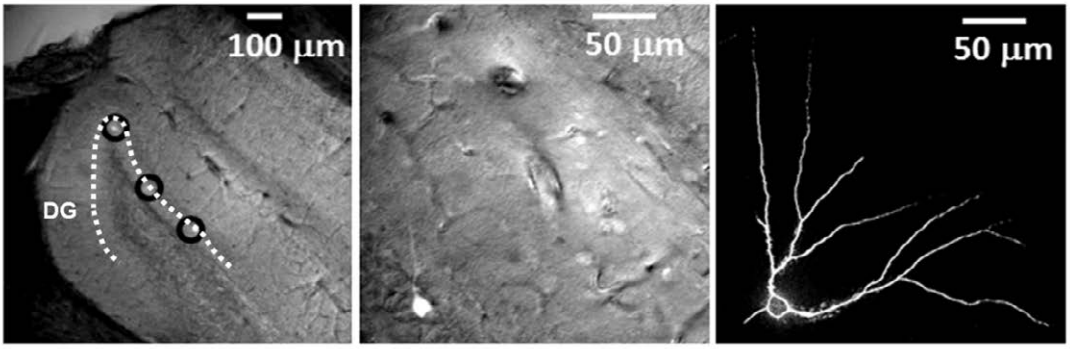

Figure 3: Brain slices contain the dentate gyrus and lucifer yellow-staining granule cells. Left panel: A part of dentate gyrus and Lucifer yellow-staining cells. Dark circles encircle lucifer yellow-staining granule cells on the brain slice. Middle panel: Magnification of a single granule cell labeled with lucifer yellow. Right panel: Z-stacks-constructed 2D image for the dendritic field of the granule cell with soma masked.

using bovine serum albumin as standards. Samples were heated for 5min at 95°C in 2× sample buffer. The electrophoretically separated proteins were transferred to PVDF membranes (Perkin-Elmer™ Life Sciences, Boston, MA, USA), blocked with 5% non-fat milk in phosphate saline-Tween-20. The membranes were then incubated overnight at 4 C with the following antibodies, including anti-ERK (1:1000), anti-pERK(1/2) (1:1000), anti-pCREB (1:1000) rabbit polyclonal antibody, and anti-CREB (1:1000) rabbit monoclonal antibody (all purchased from Cell Signaling Technology, Danvers, MA, USA). Following incubation with secondary antibody, the blots were developed with ECLTM Western blot detection kit (Amersham, Buckinghamshire, UK). The control for protein loading was performed by reprobing membranes with a monoclonal anti-β-actin antibody (Chemicon, Temecula, CA, USA).

■ Serum CORT assay

In an attempt to determine serum CORT level, mice were killed and their trunk blood collected 30 min, 3 hr, or 6 hr after the cessation of the stressor regimen in another room adjacent to the one in which they received the stressor regimen. Trunk blood samples were collected in vials and placed at room temperature for about 20 min. Blood samples were then centrifuged at 4°C for 10 min (1000 g) and serums were obtained and immediately frozen (-80°C) until assay. Serum CORT concentrations were determined using a CORT enzyme-linked immune-sorbent assay kit (Cayman Chemical Co, Ann Arbor, MI, USA) according to the manufacturer's protocols and an ELISA reader (MULTISKAN EX, Thermo Electron Corp., Finland). The intra-assay variability was 6.6 %.

■ Stress-produced and social buffering effects on mouse performance in the hippocampus-related memory tasks

For the object recognition and two versions of the Y maze task, 26 mice (10 mice from 3 cages for the "No stressor" group, 8 mice from 2 cages for the "Stressor alone" group, and 8 mice from 2 cages for the "Stressor in a group" group) were habituated to a dimly illuminated custom-made black Plexiglas box (50 cm× 50 cm× 40 cm) for 30 minutes starting at approximately 6 hours after the cessation of the stressor regimen. Two similar objects (tea cups placed upside down) were then placed on the opposite sides of the box for 10 minutes. In this 10-min acquisition trial, the time mice spent in exploring two objects was recorded. After a 5-min retention time elapsed, mice were returned to the box with one object (the one with a lesser time spent in the acquisition trial) replaced by a novel object (a ceramic tea filter) for another 10-min exploration. The time that mice spent in exploring the familiar and novel objects was recorded. The recognition percentage, ratio of the time spent exploring the novel object over the time spent exploring both objects, was used to determine the hippocampus-related memory performance in mice from the "No stressor", "Stressor alone", and "Stressor in a group" groups. Mice received the object recognition task 6-7 hours after the conclusion of the stressor regimen.

The object location task, including three habituation sessions, one sample and test phase trial, was used as previously described [36] with a minor modification. On day 1, 28 mice (10 from 3 cages for the "No stressor", 10 from 3 cages for the "Stressor alone" and 8 from 2 cages for the "Stressor in a group" groups) received three 10-min habituation sessions at approximately 2-hr intervals freely exploring in an empty Plexiglas square box (40 cm× 40 cm× 30 cm) with black walls and a bright yellow floor in a dimly lit test room. On day 2, two similar objects (tea cups with a diameter of 6 cm placed upside down) were placed in opposite corners (tea cup border was 6.8 cm away from two adjacent walls) of the box in the same dimly lit test room. Mice were allowed to freely explore the box for 10 minutes, serving as a sample phase trial and the time mice spent in exploring two objects was recorded. After a 5-min retention time elapsed, mice were returned to the box with one tea cup (the one with a lesser time spent in the sample phase trial) removed to a diagonally opposite corner (tea cup border was also 6.8 cm away from two adjacent walls), starting a 10-min test phase trial. The recognition percentage, ratio of the time spent exploring the tea cup in the new corner over the time spent exploring both tea cups, was used to determine the hippocampus-related memory performance in mice from the "No stressor", "Stressor alone", and "Stressor in a group" groups. Mice received the sample phase trial 6-7 hours after the conclusion of the stressor regimen. It was of importance to note that the box and tea cups were thoroughly cleaned between trials to stop the plausible build-up of olfactory cues.

A custom-made Y maze consisted of three identical arms symmetrical to each other on a triangular platform [37]. In the spontaneous

arm alteration version, mice were placed in the end of any random-assigned arm and allowed a 5-min free navigation in the maze at 6 hours after the conclusion of the stressor regimen. The sequence and number of all arm entries were recorded for each animal throughout the period. The sequence triads, in which all three arms were represented (including ABC, ACB, BAC, BCA, CAB, and CBA), were calculated as successful alternation to reflect the spatial working memory of the last arms entered. The percentage was then obtained from dividing the number of successful alterations by the number of possible alternations (the total number of arm entries - 2). In the exploration for the previously blocked arm version, mice were placed in the end of any random-assigned arm (start arm) and allowed to explore two arms (start and familiar arms) with one arm (unfamiliar arm) blocked for 15 min at approximately 7 hours after the conclusion of the stressor regimen. Five minutes following the 15-min exploration, mice were subjected to the end of the start arm with all arms open and the amount of time spent in the unfamiliar arm over a 5-min period was used to indicate the spatial working memory performance.

Statistical analysis

Two-way ANOVAs were employed to analyze the group (No stressor vs. Stressor alone vs. Stressor in a group) and cage differences in the total dendritic length and the number of dendritic branches of the DG granule cells as well as the number of dendritic spines/μm followed by Bonferroni's post hoc tests if appropriate. In Sholl analysis, a two-way repeated measures ANOVA was used to analyze the group (No stressor vs. Stressor alone vs. Stressor in a group) and repeated measure (distance from soma) differences in the number of intersections. One-way ANOVAs were employed to analyze the group (No stressor vs. Stressor alone vs. Stressor in a group) differences in the performance in the Y maze, object recognition and location tasks followed by Bonferroni's post hoc tests if appropriate. Likewise, a one-way ANOVA was employed to analyze the time point and group differences in serum CORT levels followed by Bonferroni's post hoc tests if appropriate. One-way ANOVAs were used to assess the group differences in the ERK and CREB phosphorylation at four time points. The levels of statistical significance were all set at $p<0.05$.

Results

■ The stressor regimen caused decreases in the number of dendritic branches and total dendritic length for each DG granule cell, while the presence of companions prevented the decreases

A two-way ANOVA revealed that group differences for the number of dendritic branches [$F(2,27)=97.23$, $p<0.0001$], while cage differences or group-cage interactions on the number of dendritic branches were not evident. Post-hoc analyses further indicated that the stressor regimen caused significant decreases in the number of dendritic branches for the existing granule cell in DG ($p<0.05$), while the presence of companions prevented such decreases **(Figure 4a)**. Likewise, a two-way ANOVA revealed group differences in the total dendritic length [$F(2,27)=44.27$, $p<0.0001$], while cage differences or group-cage interactions on the total dendritic length were not observed. Post-hoc analyses indicated that the stressor regimen produced significant decreases in the total dendritic length for the granule cells in DG ($p<0.05$), while the presence of companions effectively prevented the decreases. To further divide the granule cells into two groups, one group with only 1 primary dendrite and the other group with 2 primary dendrites, no cage differences or cage-group interactions were found. Moreover, two-way ANOVAs indicated that the stressor regimen produced significant decreases in the total dendritic length for both groups of the granule cells [$F(2,27)=42.06$, $p<0.0001$; $F(2,27)=55.18$, $p<0.0001$]. The presence of companions effectively prevented such total dendritic length decreases in the granule cells with 1 primary dendrite and with 2 primary dendrites ($p<0.05$) **(Figure 4b)**.

■ Sholl analysis revealed that the stressor regimen decreased the number of intersections from rings 3 to 19, while social buffering prevented these decreases

A one-way repeated measure ANOVA revealed that there was a main effect of group on the number of intersections [$F(2,891)=326.3$, $p<0.0001$] **(Figure 4c)**. Moreover, the distance from soma significantly affected the number of intersections [$F(26,891)=789.4$, $p<0.0001$] **(Figure 4c)**. There was a significant interaction of group and distance from soma on the number of intersections [$F(52,891)=6.73$, $p<0.0001$] **(Figure 4c)**. Post hoc analyses further showed that the stressor regimen caused significant

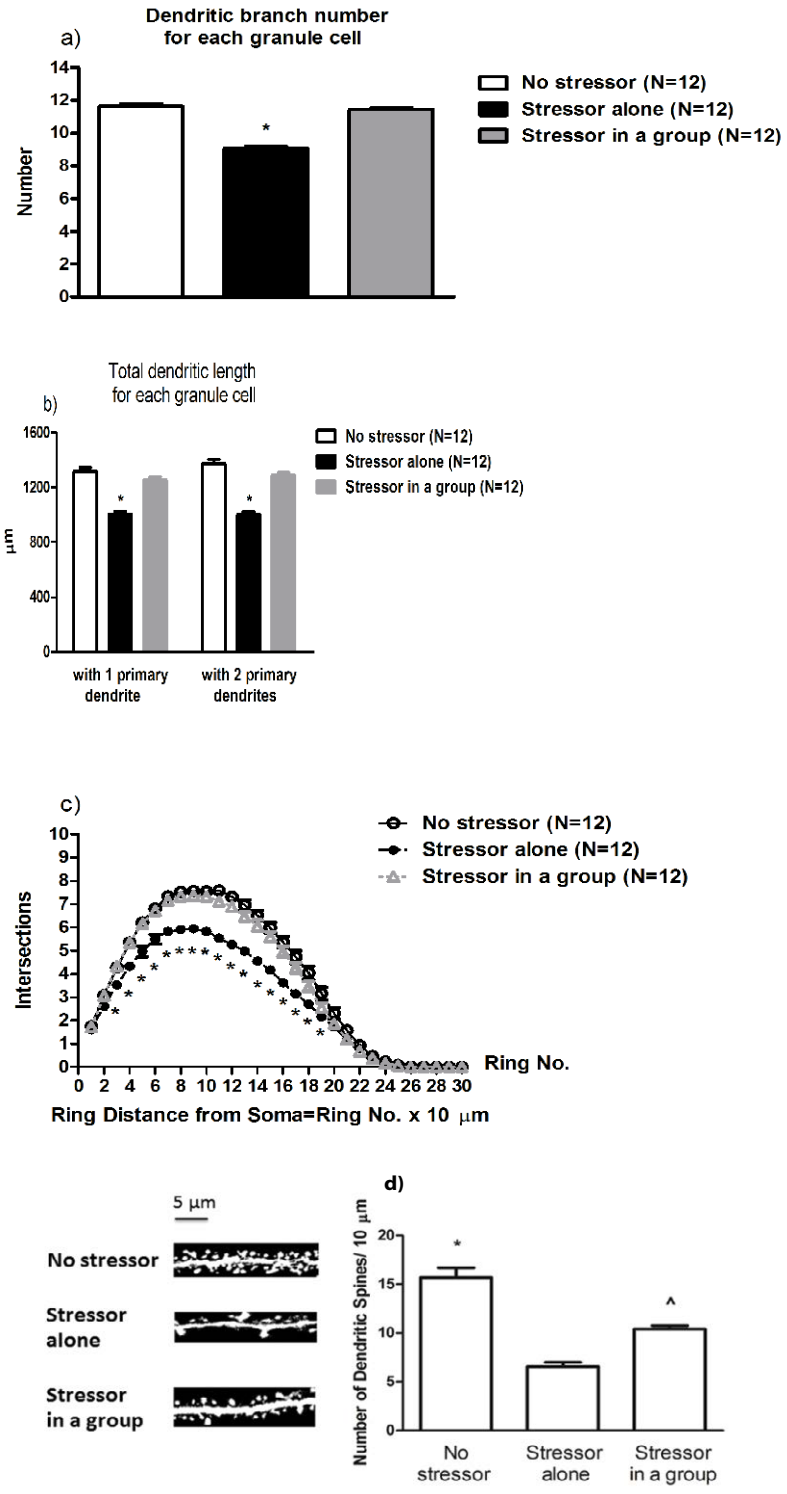

Figure 4: Dendritic measures of the DG granule cell in three groups. (a) Dendritic branch number and (b) total dendritic length of the DG granule cells with one or two primary dendrites are obtained from mice in "No stressor", "Stressor alone" and "Stressor in a group" group. *Significantly lower than "No stressor" and "Stressor in a group" group. The bar and the error bar represent the group mean and the S.E.M., respectively. (c)The number of intersections from ring 1 (10 µm from soma) to ring 30 (300 µm from soma) for the DG granule cells are plotted for the "No stressor", "Stressor alone" and "Stressor in a group" group. *Significantly lower than "No stressor" and "Stressor in a group" group. The point and the error bar represent the group mean and the S.E.M., respectively, for each ring distance. (d) Schematic representations of dendritic spines and dendritic spine density of the DG granule cells in "No stressor", "Stressor alone" and "Stressor in a group" group. *Significantly higher than the other two groups. ^Significantly higher than "Stressor alone" group. The bar and the error bar represent the group mean and the S.E.M., respectively.

decreases in the number of intersections from 30 to 190 um from soma ($p<0.05$), while the presence of companions prevented all these decreases **(Figure 4c)**. Dendritic spine density results for each mouse were summarized for "No stressor", "Stressor alone" and "Stressor in a group" group (n = 12 for each group). A two-way ANOVA revealed group differences in dendritic spine density [$F(2,27)=49.61$, $p<0.0001$], while cage differences or group-cage interactions were not noticed. Post-hoc analyses further revealed that the stressor regimen caused significant decreases in dendritic spine density of the granule cells in anterior (or dorsal) DG ($p<0.05$) **(Figure 4d)**. Moreover, such decreases in dendritic spine density of the DG granule cells were partially prevented by the presence of companions throughout the stressor regimen ($p<0.05$) (**(Figure 4d)**.

■ The stressor regimen caused hippocampus-related memory impairment, while social buffering prevented the impairment

Approximately 6-7 hours after the cessation of the stressor regimen, mice from the "Stressor alone" group demonstrated significantly lower percentage of object recognition and location tasks as compared to the "No stressor" and the "Stressor in a group" group [$F(2,23)=9.38$, $p=0.0011$; $F(2,25)=15.98$, $p<0.0001$] (Figure 5). Nonetheless, mice exhibited comparable percentages in successful alternation and time spent in unfamiliar arm in the Y maze task regardless of the exposure to the stressor regimen (Figure 5).

■ Stress rendered significant increases in serum CORT level, while social buffering did not affect the increases

While the stressor regimen rapidly stimulated CORT increases [$F(8,71)=37.93$, $p<0.0001$], the "Stressor alone" and "Stressor in a group" groups demonstrated comparable serum CORT concentrations across 6 hours (Figure 6). Interestingly, enhanced CORT level reverted to baselines at 6 hours after the conclusion of the stressor regimen (Figure 6).

■ Stress caused significant decreases in DG ERK phosphorylation, while social buffering, in part, prevented the decrease

The stressor regimen drastically caused a decrease in ERK phosphorylation (pERK/ERK) in mouse DG [$F(8,63)=17.64$, $p<0.0001$] (Figure 7a). Social buffering prevented the stressor regimen-caused decrease in ERK phosphorylation immediately after the conclusion of the stressor regimen **(Figure 7a)**. However, mice from the "Stressor in a group" and the "Stressor alone" group exhibited lower ERK phosphorylation at 0.5, 3 and 6 hours after the conclusion of the stressor regimen compared to mice receiving no stressors **(Figure 7a)**, suggesting that our stressor regimen produced a long-lasting suppression on ERK phosphorylation in DG. Since total ERK expression in three groups remained comparable and unaltered across 6 hours, these findings, taken together, implied that stressor-induced decrease in DG ERK phosphorylation was prevented by the presence of social buffering only at the time point of the end of the stressors. In contrast, the stress or social buffering did not affect total CREB or CREB phosphorylation (pCREB/CREB) across 6 hours after the conclusion of the stressor regimen **(Figure 7b)**.

Discussion

■ An acute, intense stressor causes rapid morphological changes in granule cells in hippocampal dentate gyrus

In this study, we found that a tandem stressor regimen produced rapid changes in several morphological indices of the existing granule cells in the dentate gyrus. Specifically, the stressor regimen caused significant decreases in the total dendritic length, dendritic branch number, and the size of dendritic field in the existing granule cells at 6 hours after the conclusion of the stressor regimen. Moreover, we found that such a stressor regimen caused significant decreases in dendritic spine density in dendrites of the granule cells in the anterior (or dorsal) dentate gyrus at 6 hours after the conclusion of the stressor regimen. Although chronic stress has been known to produce long-lasting dendritic atrophy in hippocampus [38], a 1-hr platform stress was also reported to cause immediate morphological changes in hippocampus [39]. In parallel with the latter report, our findings indicated that a robust stressor may indeed render morphological changes in the existing granule cells in hippocampal dentate gyrus. Our findings using an acute stress regimen have two implications in this regard. First, not only an acute, intense stress may cause rapid morphological changes in hippocampus, but such stress-caused changes may, at least, last for a time window of several hours. Second, acute and robust stress-produced long-lasting morphological changes may play a

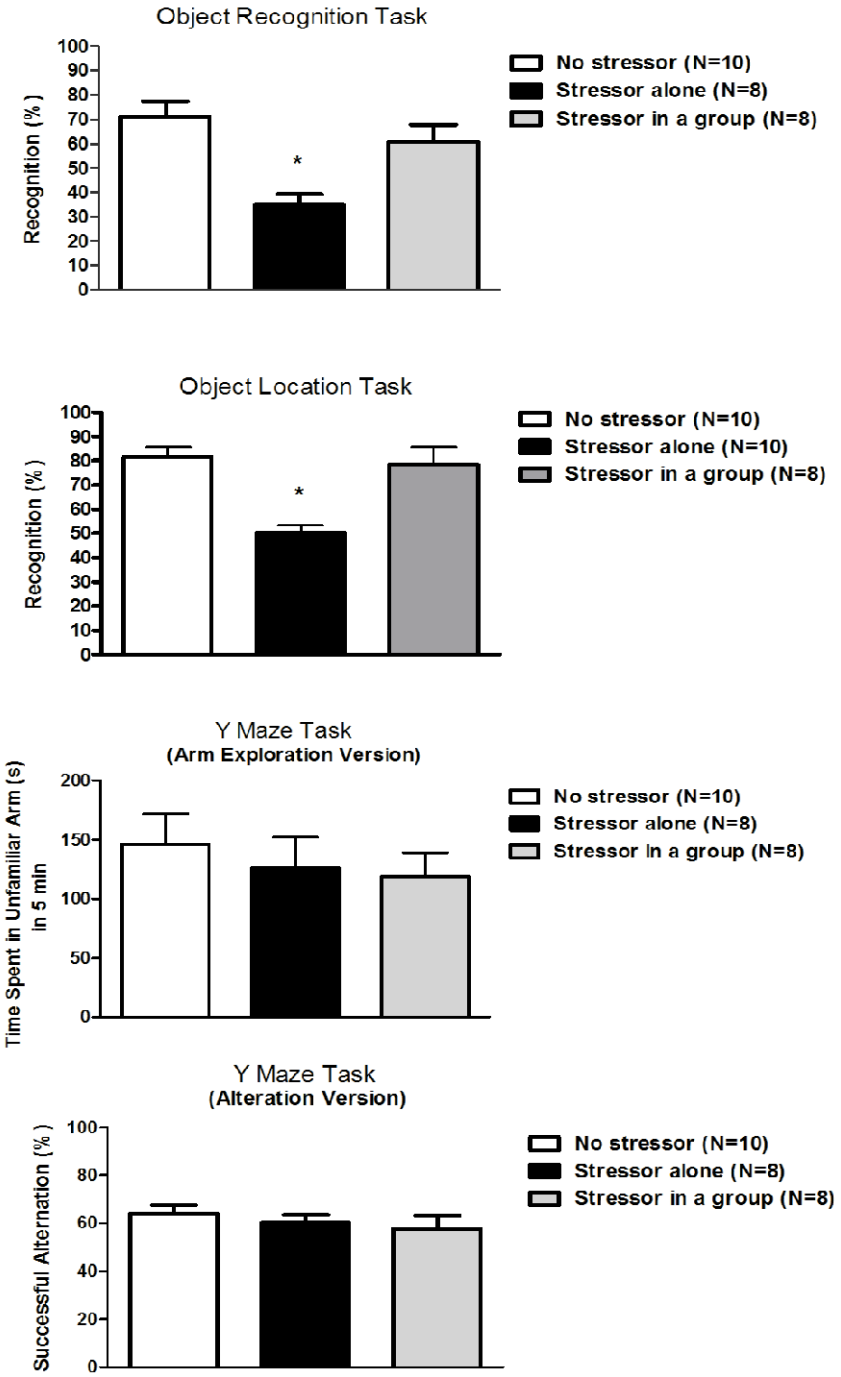

Figure 5: Impact of the stressors on hippocampus-related memory performance is plotted for three groups of mice. *Significantly lower than "No stressor" and "Stressor in a group" group. The significance levels are all set at $p<0.05$. The bar and the error bar represent the group mean and the S.E.M., respectively.

role in priming for repeated or chronic stress-induced irreversible morphological damages observed in hippocampus [40].

■ The presence of companions prevents such stressor-induced morphological changes in dentate granule cells

Although the stressor regimen caused drastic morphological changes in granule cells, the presence of companions prevented the stressor-induced decreases in most of the morphological indices. Previously, we have demonstrated that olfactory processing via activation of sensory neurons in the main olfactory epithelium may be responsible for the companions' buffering effects against the stress-caused decreases in

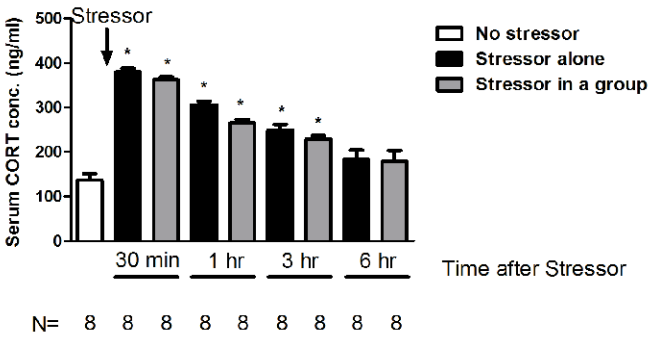

Figure 6: Impact of stressors and companions on serum CORT. The stressor regimen-produced stress rapidly increases serum CORT levels regardless of the presence of a group of three companions. *Significantly higher than the "No stressor" group. The significance levels are set at $p<0.05$. The bar and the error bar represent the group mean and the S.E.M., respectively

early neurogenesis in the dentate gyrus [41]. Such companions' odors-mediated olfactory processing may, in turn, relay the social stimulation to the dentate gyrus and stimulate local BDNF secretion in the dentate gyrus [10]. In fact, stress-induced corticosterone secretion may decrease dentate BDNF levels in a dose-dependent manner [42,43]. Dendrite complexity of the dentate granule cell has been known to be associated with the local BDNF levels [12]. Accordingly, we propose that the presence of companions may prevent the stress-induced morphological changes in dentate granule cells, in part, via the companion odor-mediated olfactory activation and reinstatement of local BDNF expression in dentate gyrus. In addition to companion-induced olfactory activation, companions' physical contact has been demonstrated to display reward-modulating effects [44-47]. Unconditioned foot shock as we used in our stressor regimen has been reported to enhance physical contact and aggressive attack in mice [48]. Whether 30-min unavoidable foot shock delivery may enhance physical contact in experimental mice and such physical contact stimulation may, in turn, prevent the stress-induced morphological changes in dentate granule cells remains to be determined.

■ The presence of companions prevents the stressor-induced decreases in certain hippocampus-related memory performances

The stressor regimen caused significant decreases in dendritic spine density of the granule cells in anterior (or dorsal) DG, while such decreases were partially prevented by the presence of companions. Dendritic spine density of the pyramidal cells in the hippocampal CA3 region has been identified to closely associate with the Y maze performance in rats [38]. In this study, we found that neither the stressor regimen nor the presence of companions affected mouse Y maze performance. These findings further suggest that neither dendritic atrophy nor reduced numbers of dendritic spines in the dentate granule cells are sufficient to induce the emergence of spatial and working memory deficits using the Y maze task.

While the stressor regimen did not affect Y maze performances, mice receiving the stressor regimen alone exhibited a lower percentage of recognition in the object recognition and location tasks as compared to mice receiving no stressor at 6-7 hours after the conclusion of the stressor regimen. Importantly, the presence of companions prevented such stress-induced decreases in the percentage of recognition in the object recognition and location tasks. Nonetheless, a recent study has demonstrated that perirhinal and medial prefrontal cortices may be more responsible for mediating the object recognition memory, while hippocampal-cortical circuits are necessary for the acquisition and retrieval of the object location memory [49]. Accordingly, we suspect that the present stressor regimen and social buffering effects may also affect neural plasticity and physiological function of perirhinal or medial prefrontal cortices.

In this study, we found that the stressor regimen caused a rapid decrease in ERK phosphorylation, while social buffering prevented such a decrease in the dentate gyrus. ERK phosphorylation plays a critical role in controlling the spine formation in primary cultured hippocampal neurons and object location memory [28,50]. Since BDNF induction may stimulate ERK phosphorylation [26-29] and the present stressor regimen has been found to produce rapid decrease in local BDNF level in DG [10,11], it is reasonable to

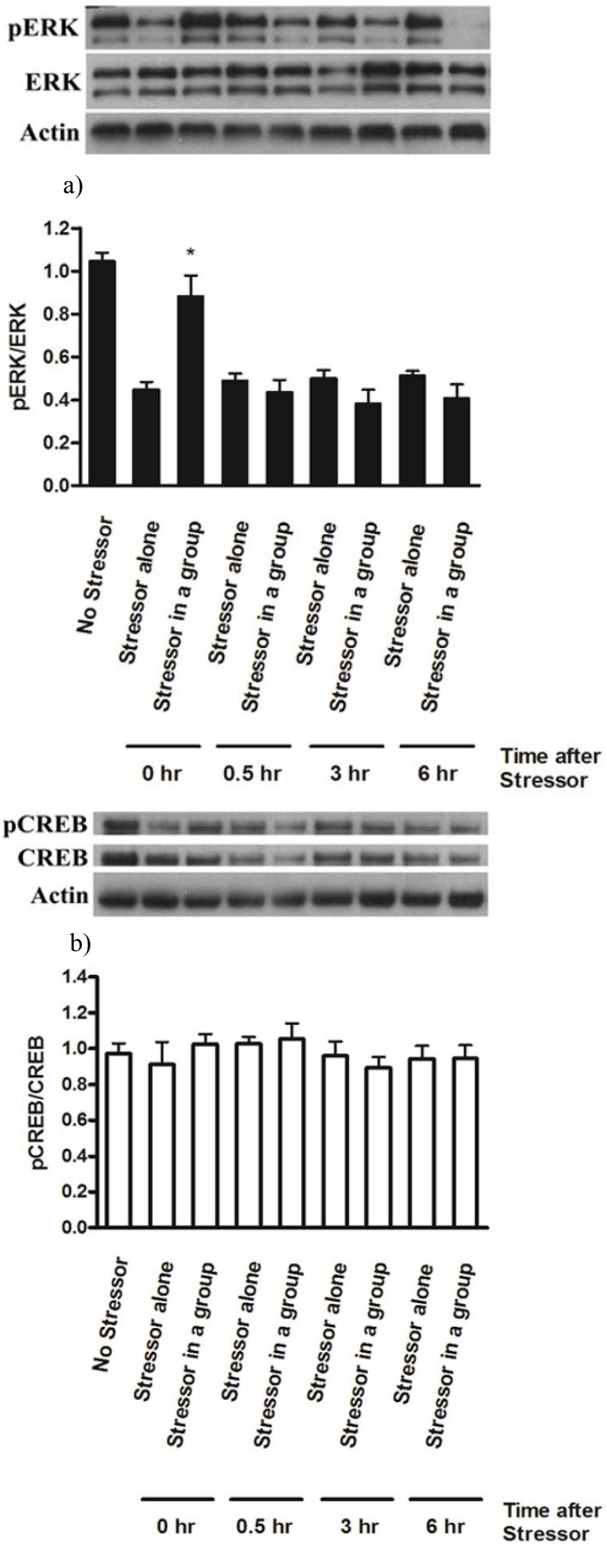

Figure 7: Impact of stressors and companions on DG ERK and CREB phosphorylation. (a) The stressor regimen-produced stress causes decreases in DG ERK phosphorylation in mice undergoing the stressor regimen alone. Social buffering effects prevent such stress-decreased ERK phosphorylation immediately after the completion of the stressor regimen. *Significantly higher than the "Stressor alone" groups. N=8 for each bar. The significance levels are set at $p<0.05$. The bar and the error bar represent the group mean and the S.E.M., respectively. (b) Stress or the presence of companions does not affect CREB phosphorylation. N=8 for each bar. The bar and the error bar represent the group mean and the S.E.M., respectively.

speculate that the stress-caused rapid decreases in BDNF secretion and/or ERK phosphorylation may be involved in priming object location memory impairment in mice receiving the stressor regimen alone.

■ Roles of stress-increased CORT and -decreased local BDNF secretion in mediating the granule morphological changes

We replicated our previous finding [9] that the stressor regimen rapidly enhanced serum corticosterone levels regardless of the presence of companions. Since stress-enhanced corticosterone secretions have been shown to be necessary to cause atrophy of dendrites in hippocampal neurons [4-7], the stressor-stimulated corticosterone secretion likely plays a role in initiating the morphological changes in the existing granule cells. Variations in the morphological changes in the existing granule cells between mice receiving the stressor alone versus in a group could be primarily due to the social buffering effects. In fact, we have reported that social buffering-produced local BDNF replenishment could be responsible for its effect on reversing the corticosterone-decreased early neurogenesis in the dentate gyrus [10,11]. Similarly, a recent report has documented that local BDNF levels are critical in predicting the stress-produced morphological changes in the dentate gyrus [51]. Therefore, social buffering-stimulated local BDNF replenishment could prevent not only the stress-induced decrease in early neurogenesis but the corticosterone-initiated morphological changes in the dentate granule cells.

■ A role of local ERK phosphorylation in mediating the stress and social buffering effects on granule morphological indices and hippocampus-related memories

Approximately 6-7 hours after the conclusion of the stressor regimen, decreases in morphological indices of the existing DG granule cells and hippocampus-related memory performance were evident in mice displaying stressor-caused immediate decrease in local ERK phosphorylation. In parallel with this finding, a recent report reveals that a chronic mild stressor enhances serum corticosterone secretion but reduces hippocampal ERK phosphorylation, and working memory performance in a rat model [52]. The same report also points out that such chronic mild stressor reduces the CREB phosphorylation in the hippocampus [52]. Nonetheless, we found that our stressor regimen did not affect local CREB phosphorylation in mouse dentate gyrus regardless of the presence of companions. This discrepancy could arise from species, stress protocol, brain region and observation timing differences between their study and ours. In fact, one line of evidence has indicated that ERK activation may mediate protein synthesis and neural plasticity independent of activation of CREB [53]. And ERK is, after all, one of the many intracellular signaling molecules responsible for stimulating CREB phosphorylation. We, accordingly, speculate that some transcription factors other than CREB could be involved in the stressor-induced decreases in de novo protein synthesis and subsequent morphological plasticity of the DG granule cells and memory deficits. Moreover, mice receiving the stressor regimen alone or in a group exhibited comparable DG ERK phosphorylation magnitudes at 0.5, 3 and 6 hours after the conclusion of the stressor regimen and all lower than those in mice receiving no stressor. Likewise, mice receiving the stressor regimen displayed increases in serum corticosterone secretion regardless of the presence of the companions. However, only mice receiving the stressor regimen alone demonstrated significant decreases in morphological indices of the DG granule cells and DG-related memory. Thus, we alternatively suspect that stress-induced increase in corticosterone secretion followed by decrease in local ERK phosphorylation might not be sufficient to cause morphological changes in the DG granule cells or DG-related memory deficits. In fact, a recent report has revealed that corticosterone level plays a minor role in mediating combined acute and chronic stress-mediated changes in ERK phosphorylation in the dentate gyrus [54], suggesting a dissociation of serum corticosterone secretion and ERK phosphorylation in DG.

Our previous reports have demonstrated that the present stressor regimen causes a rapid decrease in BDNF, but not TrkB, expression in DG [10,11]. Meanwhile, social buffering effectively reinstates such stress-induced decreases in local BDNF expression [10]. It has been known that BDNF-induced activation of TrkB, a BDNF receptor, may lead to downstream ERK phosphorylation in hippocampus [55]. In this study, we found that the stressor regimen induced an immediate decrease in ERK phosphorylation in the dentate

gyrus, while social buffering prevented such immediate decreases. The stressor regimen or social buffering did not affect total ERK expression, suggesting that the stressor regimen or social buffering does not alter the synthesis and degradation of local ERK protein. Thus, mice receiving the stressors alone were expected to express less phosphorylated ERK as compared to mice receiving the stressor regimen in a group immediately after the conclusion of the stressor regimen. And the former, not the latter, displayed evident dendritic atrophy in DG granule cells and DG-related memory deficits. Thus, immediate decreases in DG ERK phosphorylation following the present stressor regimen could be one of the underlying mechanisms in producing social buffering effects against stress-induced decreases in DG granule morphological indices and DG-related memory. Paradoxically, mice receiving the stressor regimen alone or in a group exhibited comparable DG ERK phosphorylation magnitudes on the remaining time points after the stressor regimen. Further work is needed to test whether BDNF-TrkB-induced signaling to ERK activation is actually responsible for the stress-induced changes and social buffering effects on granule cell morphology and DG-related memory performance.

■ Granule morphological changes and hippocampus-related memory performance

Although extremely low circulating levels of corticosterone may render small and simple dendritic trees of the granule cells in the dentate gyrus, the voltage-dependent calcium currents, primarily generated from distal dendrites of these cells, are not altered [56]. Likewise, a recent report indicates that corticosterone does not change high-voltage activated calcium currents or calcium channel subunit expression in the dentate gyrus [57]. These lines of evidence suggest that, despite atrophy of the dendritic field of the dentate granule cells, the chemical transmission and basal neuronal activity might not be altered. In this study, we found that mice receiving a tandem stressor regimen demonstrated shorter length of dendrites, fewer dendritic branches and smaller dendritic fields in the dentate granule cells as well as functional deficit in spatial working memory. However, social buffering prevented most of these stress-produced morphological changes in the granule cells and the deficit in the spatial working memory. Even though firing-dependent calcium influx could be intact in the dendrites of the existing granule cells, stress-produced decreases in dendritic field in these cells may cause observable cognitive and behavioral deficits pertaining to dentate function.

A growing body of evidence indicate that germ-free mice may serve as an intriguing animal model for studying the pathologies of anxiety disorders because these mice are prone to display exaggerated HPA axis responses to acute stressors, reduced anxiety-like behaviors, and cognitive and behavioral deficits [58-62]. Interestingly, a recent study indicates that the dendritic trees of dentate granule cells of germ-free mice are less branched as compared to conventionally colonized mice [63]. Moreover, germ-free and conventionally colonized mice display comparable spine density in the dentate gyrus [63]. In parallel with these findings, we thereby report that shrinkage of dendritic field, but not spine density, in granule cells are closely related to functional deficits of the dentate gyrus.

Conclusions

These results, taken together, prompt us to conclude that acute, robust stress may cause rapid morphological changes on the existing granule cells in the dentate gyrus and object location memory deficits. Social buffering prevents most of these stress-produced effects probably by modulating the BDNF-induced ERK phosphorylation in the local area. The presence of companions may afford an intervention advance in preventing stress-produced acute impact on the granule cell morphology and hippocampal function.

Conflict of interest

The authors declare no conflict of interest.

Acknowledgments

This research was, in part, supported by ROC Ministry of Science and Technology (MOST) grants 103-2410-H-006 -028 -MY3 to L.Y., and 102-2221-E-309-005 to C.G.C., Chen-Yi Joint Program grant NCKUEDA 10514 to L.Y. and S-N.Y. We would like to extend our deepest appreciation for Dr. G.C. Wagner's reading and proofing of the manuscript.

References

1. Sousa N, Almeida OF. Corticosteroids: sculptors of the hippocampal formation. *Rev. Neurosci* 13(1), 59-84 (2002).
2. Martinez-Claros M, Steinbusch HW, van Selm A, *et al.* Adrenalectomy and corticosterone replacement differentially alter CA3 dendritic morphology and new cell survival in the adult rat hippocampus. *J. Chem. Neuroanat* 48(1), 23-28 (2013).
3. Magarinos AM, McEwen BS. Stress-induced atrophy of apical dendrites of hippocampal CA3c neurons: comparison of stressors. *Neuroscience* 69(1), 83–88 (1995a).
4. Magarinos AM, McEwen BS. Stress-induced atrophy of apical dendrites of hippocampal CA3c neurons: involvement of glucocorticoid secretion and excitatory amino acid receptors. *Neuroscience* 69(1), 89–98 (1995b).
5. Woolley CS, Gould E, McEwen BS. Exposure to excess glucocorticoids alters dendritic morphology of adult hippocampal pyramidal neurons. *Brain. Res* 531(1-2), 225–231 (1990).
6. Watanabe Y, Gould E, McEwen BS. Stress induces atrophy of apical dendrites of hippocampal CA3 pyramidal neurons. *Brain. Res* 588(2), 341–345 (1992).
7. Galea LA, McEwen BS, Tanapat P, *et al.* Sex differences in dendritic atrophy of CA3 pyramidal neurons in response to chronic restraint stress. *Neuroscience* 81(3), 689–697 (1997).
8. Sloviter RS, Valiquette G, Abrams GM, *et al.* Selective loss of hippocampal granule cells in the mature rat brain after adrenalectomy. *Science* 243(4890), 535–538 (1989).
9. Cherng CG, Lin PS, Chuang JY, *et al.* Presence of conspecifics and their odor-impregnated objects reverse stress-decreased proliferated neuroblasts in mouse dentate gyrus. *J. Neurochem* 112(5), 1138-1146 (2010).
10. Tzeng WY, Chuang JY, Lin LC, *et al.* Companions reverse stressor-induced decreases in proliferated neuroblasts and cocaine conditioning possibly by restoring BDNF and NGF levels in dentate gyrus. *Psychoneuroendocrinology* 38(1), 425-437 (2013).
11. Tzeng WY, Chen L-H, Cherng CG, *et al.* Sex differences and the modulating effects of gonadal hormones on basal and the stressor-decreased newly proliferative cells and neuroblasts in dentate gyrus. *Psychoneuroendocrinology* 42(1), 24-37 (2014).
12. Tolwani RJ, Buckmaster PS, Varma S, *et al.* BDNF overexpression increases dendrite complexity in hippocampal dentate gyrus. *Neuroscience* 114(3), 795-805 (2002).
13. Gooney M, Shaw K, Kelly A, *et al.* Long-term potentiation and spatial learning are associated with increased phosphorylation of TrkB and extracellular signal-regulated kinase (ERK) in the dentate gyrus: evidence for a role for brain-derived neurotrophic factor. *Behav. Neurosci* 116(3), 455-463 (2002).
14. Holm MM, Nieto-Gonzalez JL, Vardya I, *et al.* Mature BDNF, but not proBDNF, reduces excitability of fast-spiking interneurons in mouse dentate gyrus. *J. Neurosci* 29(40), 12412-12418 (2009).
15. Ying SW, Futter M, Rosenblum K, *et al.* Brain-derived neurotrophic factor induces long-term potentiation in intact adult hippocampus: requirement for ERK activation coupled to CREB and upregulation of Arc synthesis. *J. Neurosci* 22(5), 1532-1540 (2002).
16. Fahlman CS, Bickler PE, Sullivan B, *et al.* Activation of the neuroprotective ERK signaling pathway by fructose-1,6-bisphosphate during hypoxia involves intracellular Ca^{2+} and phospholipase C. *Brain. Res* 958(1), 43-51 (2002).
17. Lee S, Yang M, Kim J, *et al.* Involvement of BDNF/ERK signaling in spontaneous recovery from trimethyltin-induced hippocampal neurotoxicity in mice. *Brain Res. Bull* 121(1), 48-58 (2016).
18. Kesner RP, Hunsaker MR, Warthen MW. The CA3 subregion of the hippocampus is critical for episodic memory processing by means of relational encoding in rats. *Behav. Neurosci* 122(6), 1217-1225 (2008).
19. Cai L, Gibbs RB, Johnson DA. Recognition of novel objects and their location in rats with selective cholinergic lesion of the medial septum. *Neurosci. Lett* 506(2), 261-265 (2012).
20. Wiescholleck V, Manahan-Vaughan D. Persistent deficits in hippocampal synaptic plasticity accompany losses of hippocampus-dependent memory in a rodent model of psychosis. *Front. Integr. Neurosci* 7(1), 12 (2013).
21. Bustamante C, Valencia M, Torres C, *et al.* Effects of a single course of prenatal betamethasone on dendritic development in dentate gyrus granular neurons and on spatial memory in rat offspring. *Neuropediatrics* 45(6), 354-361 (2014).
22. Ferreira-Vieira TH, Bastos CP, Pereira GS, *et al.* A role for the endocannabinoid system in exercise-induced spatial memory enhancement in mice. *Hippocampus* 24(1), 79-88 (2014).
23. O'Callaghan R, Ohle R, Kelly AM. The effects of forced exercise on hippocampal plasticity in the rat: A comparison of LTP, spatial- and non-spatial learning. *Behav. Brain. Res* 176(2), 362–366 (2007).
24. Griffin EW, Bechara RG, Birch AM, *et al.* Exercise enhances hippocampal-dependent learning in the rat: evidence for a BDNF-related mechanism. *Hippocampus* 19(10), 973-980 (2009).
25. Bechara RG, Kelly AM. Exercise improves object recognition memory and induces BDNF expression and cell proliferation in cognitively enriched rats. *Behav. Brain. Res* 245(1), 96-100 (2013).
26. Rendeiro C, Vauzour D, Kean RJ, *et al.* Blueberry supplementation induces spatial memory improvements and region-specific regulation of hippocampal BDNF mRNA expression in young rats. *Psychopharmacology (Berl)* 223(3), 319-330 (2012).
27. Callaghan CK, Kelly AM. Neurotrophins play differential roles in short and long-term recognition memory. *Neurobiol. Learn. Mem* 104(1), 39-48 (2013).
28. Tuscher JJ, Fortress AM, Kim J, *et al.* Regulation of object recognition and object placement by ovarian sex steroid hormones. *Behav. Brain. Res* 285(1), 140-157 (2015).
29. Lim S, Moon M, Oh H, *et al.* Ginger improves cognitive functions *via* NGF-induced ERK/CREB activation in the hippocampus of the mouse. *J. Nutr. Biochem* 25(10), 1058-1065 (2014).
30. Phillips LL, Pollack AE, Stewart O. Protein synthesis in the neutrophil of the rat dentate gyrus during synapse development. *J. Neurosci. Res* 26(1), 474-482 (1990).
31. Qin M, Entezam A, Usdin K, *et al.* A mouse model of the fragile X premutation: Effects on behavior, dendrite morphology, and regional rates of cerebral protein synthesis. *Neurobiol. Diseas* 42(1), 85-98 (2011).
32. Huang TY, Lin LS, Cho KC, *et al.* Chronic treadmill exercise in rats delicately alters the Purkinje cell structure to improve motor performance and toxin resistance in the cerebellum. *J. Appl. Physiol* 113(6), 889-895 (2012).
33. Zhao C, Teng EM, Summers RG, *et al.* Distinct Morphological Stages of Dentate Granule Neuron Maturation in the Adult Mouse Hippocampus. *J. Neurosci* 26(1), 3-11 (2006).
34. Zhao C, Warner-Schmidt J, Duman RS, *et al.* Electroconvulsive seizure promotes spine maturation in newborn dentate granule cells in adult rat. *Dev. Neurobiol* 72(6), 937-942 (2012).
35. Halasy K, Somogyi P. Subdivisions in the multiple GABAergic innervation of granule cells in the dentate gyrus of the rat hippocampus. *Eur. J. Neurosci* 5(5), 411-429 (1993).

36. De Rosa R, Garcia AA, Braschi C, *et al.* Intranasal administration of nerve growth factor (NGF) rescues recognition memory deficits in AD11 anti-NGF transgenic mice. *Proc. Nat. Acad. Sci. USA* 102(10), 3811–3816 (2005).

37. Cherng CG, Tsai CW, Tsai YP, *et al.* Methamphetamine-disrupted sensory processing mediates conditioned place preference performance. *Behav. Brain. Res* 182(), 103-108 (2007).

38. Conrad CD, Galea LAM, Kuroda Y, *et al.* Chronic stress impairs rat spatial memory on the Y maze, and this effect is blocked by tianeptine treatment. *Behav. Neurosci* 110(6), 1321-1334 (1996).

39. Sebastian V, Estil JB, Chen D, *et al.* Acute physiological stress promotes clustering of synaptic markers and alters spine morphology in the hippocampus. *PLoS One* 8(10), e79077 (2013).

40. Magarinos AM, McEwen BS, Flugge G, *et al.* Chronic psychosocial stress causes apical dendritic atrophy of hippocampal CA3 pyramidal neurons in subordinate tree shrews. *J. Neurosci* 16(10), 3534-3540 (1996).

41. Cherng CF, Chang CP, Su CC, *et al.* Odors from proximal species reverse the stress-decreased proliferated neuroblasts via main olfactory processing. *Behav. Brain. Res* 229(1), 106-112 (2012).

42. Gronli J, Bramham C, Murison R, *et al.* Chronic mild stress inhibits BDNF protein expression and CREB activation in the dentate gyrus but not in the hippocampus proper. *Pharm. Biochem. Behav* 85(4), 842-849 (2006).

43. Schaaf MJM, de Jong J, de Kloet, *et al.* Downregulation of BDNF mRNA and protein in the rat hippocampus by corticosterone. *Brain. Res* 813(1), 112-120 (1998).

44. Fritz M, Rawas RE, Salti A, *et al.* Reversal of cocaine-conditioned place preference and mesocorticolimbic Zif268 expression by social interaction in rats. *Addict. Biol* 16(2), 273-284 (2011).

45. Peartree NA, Hood LE, Thiel KJ, *et al.* Limited physical contact through a mesh barrier is sufficient for social reward-conditioned place preference in adolescent male rats. *Physiol. Behav* 105(3), 749–756 (2012).

46. Tzeng W-Y, Cherng CG, Wang S-W, *et al.* Familiar companions diminish cocaine conditioning and attenuate cocaine-stimulated dopamine release in the nucleus accumbens. *Behav. Brain. Res* 306(1), 146–153 (2016).

47. Pinheiro BS, Seidl SS, Habazettl E, *et al.* Dyadic social interaction of C57BL/6 mice versus interaction with a toy mouse: conditioned place preference/aversion, substrain differences, and no development of a hierarchy. *Behav. Pharmacol* 27(2-3 Spec Issue), 279-288 (2016).

48. Nath C, Gulati A, Dhawan KN, *et al.* Evidence for central histaminergic mechanism in foot shock aggression. *Psychopharmacology* 76(3), 228–231 (1982).

49. Barker GR, Warburton EC. Object-in-place associative recognition memory depends on glutamate receptor neurotransmission within two defined hippocampal-cortical circuits: a critical role for AMPA and NMDA receptors in the hippocampus, perirhinal, and prefrontal cortices. *Cereb. Cortex* 25(2), 472-481 (2015).

50. Yoon DH, Yoon S, Kim D, *et al.* Regulation of dopamine D2 receptor-mediated extracellular signal-regulated kinase signaling and spine formation by GABAA receptors in hippocampal neurons. *Neurosci. Lett* 586(1), 24-30 (2015).

51. Cohen H, Kozlovsky N, Matar MA, *et al.* Distinctive hippocampal and amygdalar cytoarchitectural changes underlie specific patterns of behavioral disruption following stress exposure in an animal model of PTSD. *Eur. Neuropsychopharmacology* 24(12), 1925-1944 (2014).

52. Liu D, Zhang Q, Gu J, *et al.* Resveratrol prevents impaired cognition induced by chronic unpredictable mild stress in rats. *Prog. Neuro-Psychopharm. Biol. Psychiat* 49(1), 21-29 (2014).

53. Panja D, Kenney JW, D'Andrea L, *et al.* Two-stage translational control of dentate gyrus LTP consolidation is mediated by sustained BDNF-TrkB signaling to MNK. *Cell. Rep* 9(4), 1430-1445 (2014).

54. Ferland CL, Harris EP, Lam M, *et al.* Facilitation of the HPA axis to a novel acute stress following chronic stress exposure modulates histone acetylation and the ERK/MAPK pathway in the dentate gyrus of male rats. *Endocrinology* 155(8), 2942-2952 (2014).

55. Gooney M, Lynch MA. Long-term potentiation in the dentate gyrus of the rat hippocampus is accompanied by brain-derived neurotrophic factor-induced activation of TrkB. *J. Neurochem* 77(5), 1198-1207 (2001).

56. Wossink J, Harst J, Mayboroda O, *et al.* Morphological and functional properties of rat dentate granule cells after adrelectomy. *Neuroscience* 108(2), 263-272 (2001).

57. van Gemert NG, Carvalho DM, Karst H, *et al.* Dissociation between rat hippocampal CA1 and dentate gyrus cells in their response to corticosterone: effects on calcium channel protein and current. *Endocrinology* 150(10), 4615-4624 (2009).

58. Sudo N, Chida Y, Aiba Y, *et al.* Postnatal microbial colonization programs the hypothalamic-pituitary-adrenal system for stress response in mice. *J. Physiol* 558(1), 263–275 (2004).

59. Heijtz RD, Wang S, Anuar F, *et al.* Normal gut microbiota modulates brain development and behavior. *Proc. Nat. Acad. Sci. USA* 108(7), 3047–3052 (2011).

60. Neufeld KM, Kang N, Bienenstock J, *et al.* Reduced anxiety-like behavior and central neurochemical change in germ-free mice. *Neurogastroent. Motil* 23(3), 255–265 (2011).

61. Clarke G, Grenham S, Scully P, *et al.* The microbiome-gut-brain axis during early life regulates the hippocampal serotonergic system in a sex-dependent manner. *Mol. Psychiatr* 18(6), 666–673 (2013).

62. Desbonnet L, Clarke G, Shanahan F, *et al.* Microbiota is essential for social development in the mouse. *Mol. Psychiatr* 19(2), 146–148 (2014).

63. Luczynski P, Whelan SO, O'Sullivan C, *et al.* Adult microbiota-deficient mice have distinct dendritic morphological changes: differential effects in the amygdala and hippocampus. *Eur. J. Neurosci* 44(9), 2654-2666 (2016).